Scheme IV[a]

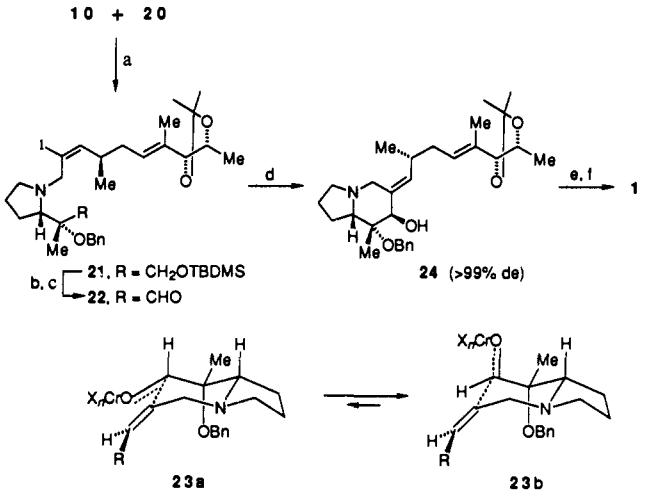

[a] (a) *i*-Pr_2NEt, THF, room temperature; (b) Bu_4NF, THF, room temperature; (c) $(COCl)_2$, DMSO, Et_3N, CH_2Cl_2, -78 °C; (d) $CrCl_2$ (5 equiv), $NiCl_2$ (2.5 mol %), DMF, room temperature; (e) 3 N HCl/THF, room temperature; (f) Li, NH_3/THF, -78 °C.

The synthesis of the optically active pyrrolidine fragment is shown in Scheme II. Deprotection of *N*-Boc-protected (*S*)-2-acetylpyrrolidine **4** with trifluoroacetic acid (3 equiv) by the known procedure[3] afforded the pyrrolidine trifluoroacetate salt, which was immediately treated with excess 2-lithio-1,3-dithiane to produce the tertiary alcohol **5** (54% from **4**) as a single diastereomer consistent with a chelation-controlled transition state. Compound **5** was converted to **6** (68%) via transformation of the cyclic dithioacetal into the corresponding dimethyl acetal with methanol and $Hg(ClO_4)_2$. After blocking of the amino group by the cyanomethyl group,[8] O-benzylation of the tertiary alcohol was effected by treating with benzyl bromide and KH[9] to produce **7** (81%), which was then converted to the carbamate **8** (75%) via deblocking of the cyanomethyl group ($AgNO_3$) and N-protection by the Cbz group. Compound **8** was further transformed into **9** (97%) through acetal hydrolysis and $NaBH_4$ reduction of the resulting aldehyde. Silylation of **9** and hydrogenolytic removal of the Cbz group resulted in **10** (80% from **9**).

The side chain segment **20** was elaborated from the D-4-deoxythreose derivative **11**[10] as outlined in Scheme III. Grignard reaction (MeMgBr, THF) followed by PCC oxidation provided the methyl ketone **12** (73% overall yield), which was transformed to the *E* olefin **13** (84%) by Horner-Emmons condensation with a nice *E*:*Z* ratio of 96:4. The bromide **14**, obtained from **13** (DIBALH, then CBr_4/PPh_3) in 91% yield, was subjected to C_2 homologation based on Evans alkylation,[11] which provided **15** (83%) with virtually complete diastereoselective creation of the *R* stereogenic center at C-11. Reductive removal of the oxazolidine auxiliary on **15** with $LiAlH_4$, followed by Swern oxidation and treatment of the resultant aldehyde with CBr_4/PPh_3, furnished the dibromide **16** in 70% overall yield from **15**. Compound **16** was converted to the hydroxyalkyne **17** in 92% yield by treatment with BuLi (2 equiv) and paraformaldehyde. Palladium-catalyzed hydrostannation [Bu_3SnH, 2 mol % $PdCl_2(PPh_3)_2$, room temperature][12] of **17** provided full stereocontrol for the (tributylstannyl)alkene **18** (93%)[13] with correct *E* olefin geometry.[14] Upon exposure of **18** to iodine (CH_2Cl_2, room temperature), iododestannylation smoothly proceeded to give exclusively the (*E*)-iodoalkene **19**, which was then converted to the allylic bromide **20** in excellent yield (96% from **18**).

Construction of the alkylideneindolizidine ring began with coupling of **10** and **20** in the presence of Hünig base to provide **21** in 70% yield (Scheme IV). Desilylation of **21** followed by Swern oxidation afforded the aldehyde **22** (81%). Intramolecular cyclization of **22** was successfully achieved by application of mild coupling conditions (5 equiv of $CrCl_2$, 2.5 mol % $NiCl_2$, DMF, room temperature) with virtually complete stereocontrol, giving rise to **24** in 79% yield. This cyclization through the alkenylchromium(III) intermediate (**2** in Scheme I) generated with Ni(II) catalyst via transmetalation led to both formation of the 6-(*E*)-alkylideneindolizidine and introduction of the axial 7β-hydroxy group at the same time in *a single operation*. The remarkably high degree of stereoselectivity leading to **24** may be explained by examination of two chair-like transition states, **23a** and **23b**, the former of which would be destabilized owing to an allylic 1,3-strain[15] between the equatorial chromium alkoxide and the olefin. The preferred transition state **23b** leads to the requisite axial 7-hydroxy group.

Finally, sequential removal of the isopropylidene protecting group (3 N HCl, THF) and the benzyl group (Li, NH_3/THF) provided (+)-allopumiliotoxin 339A (**1**) in 71% overall yield. Synthetic **1** had $[\alpha]^{28}_D$ +38.8° (*c* 0.5, MeOH) [lit.[4] $[\alpha]^{25}_D$ +29.4° (*c* 1.0, MeOH)], $[\alpha]^{28}_D$ +72.4° (*c* 0.66, $CHCl_3$) [lit.[5] $[\alpha]^{23}_D$ +68.2° (*c* 0.5, $CHCl_3$)] and exhibited spectral data (^1H and ^{13}C NMR) identical with those reported[4] for the natural product.

In conclusion, a new, highly regio- and stereocontrolled approach for the synthesis of allopumiliotoxin 339A has been developed. Our methodology based on an intramolecular chromium(II)-mediated cyclization should prove an efficient tool in the synthesis of the allo series of pumiliotoxins.

(6) (a) Rowley, M.; Kishi, Y. *Tetrahedron Lett.* **1988**, *29*, 4909. (b) Schreiber, S. L.; Meyers, H. V. *J. Am. Chem. Soc.* **1988**, *110*, 5198.
(7) Takai, K.; Tagashira, M.; Kuroda, T.; Oshima, K.; Utimoto, K.; Nozaki, H. *J. Am. Chem. Soc.* **1986**, *108*, 6048.
(8) Lett, R. M.; Overman, L. E.; Zablocki, J. *Tetrahedron Lett.* **1988**, *29*, 6541.
(9) Attempts at O-protection of the cyclic dithioketal **5** after Cbz N-protection were unsuccessful, suggesting that the *tert*-hydroxyl group in **5** is severely hindered.
(10) Servi, S. *J. Org. Chem.* **1985**, *50*, 5865. Fronza, G.; Fuganti, C.; Grasselli, P.; Marinoni, G. *Tetrahedron Lett.* **1979**, 3883.
(11) Evans, D. A.; Ennis, M. D.; Mathre, D. J. *J. Am. Chem. Soc.* **1982**, *104*, 1737.
(12) Zhang, H. X.; Guibé, F.; Balavoine, G. *J. Org. Chem.* **1990**, *55*, 1857.
(13) This reaction was accompanied by the formation of a small amount (4% yield) of the 3-tributylstannyl regioisomer.
(14) The ^1H NMR spectrum of **18** shows a coupling constant of 35 Hz between Sn and the proton at C-3, proving their *E* relationship.
(15) (a) Johnson, F. *Chem. Rev.* **1968**, *68*, 375. (b) Hoffmann, R. W. *Chem. Rev.* **1989**, *89*, 1841.

Dynamic Interpretation of NMR Data: Molecular Dynamics with Weighted Time-Averaged Restraints and Ensemble *R*-Factor

Uli Schmitz, Anil Kumar, and Thomas L. James*

Department of Pharmaceutical Chemistry
University of California
San Francisco, California 94143-0446

Received August 3, 1992
Revised Manuscript Received October 15, 1992

Determination of biomolecular structure in solution via multidimensional NMR and modeling with distance geometry and restrained molecular dynamics (rMD) generally results in a single structure in accord with structural constraints, i.e., interproton distances extracted from nuclear Overhauser enhancement (NOE) spectra and torsion angles arising from coupling constants. With rapid conformational fluctuations, constraints are time-averaged, with the time scale and nonlinear averaging being different for torsion angles and distances. Conceivably then, there is no single energetically reasonable structure that would fit all structural data simultaneously as demonstrated for the peptide antamanide.[1] A

* Author to whom correspondence should be addressed: telephone (415) 476-1569 or FAX (415) 476-0688.
(1) Kessler, H.; Griesinger, C.; Lautz, J.; Müller, A.; van Gunsteren, W. F.; Berendsen, H. J. C. *J. Am. Chem. Soc.* **1988**, *110*, 3393-3396.

0002-7863/92/1514-10654$03.00/0

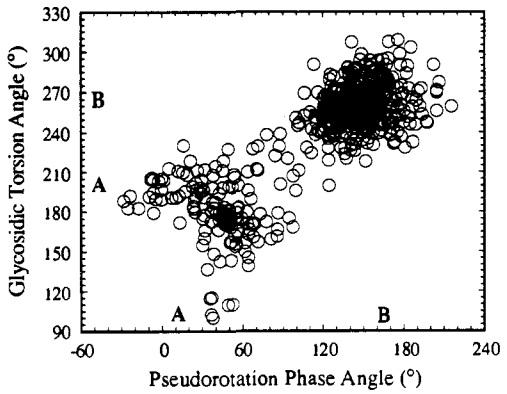

Figure 1. Correlation between glycosidic torsion angle χ and pseudorotation angle P for residue A6 in [d(GTATAATG)]·[d(CATATTAC)]. Data are from 400 snapshots taken every 0.25 ps during the last 100 ps of a 120-ps standard rMD simulation (■) and a 120-ps MD-tar simulation (○). Symbols A and B denote values of the parameters for A- or B-DNA.

dynamic interpretation of NMR-derived constraints in MD simulations has been suggested by Torda et al.[2,3] The NOE distance term in the force field was modified such that the distance between any two protons and the associated penalty is monitored as a running average with exponential weighting to emphasize more recent snapshots during a rMD trajectory. This option of running molecular dynamics is now in the AMBER program suite.[4] In a theoretical study, MD-tar was compared with conventional rMD for an idealized set of experimental distances derived from a long unrestrained MD simulation on a hexanucleotide. Even though both methods yielded the same gross morphology, MD-tar seemed to reflect the inherent flexibility much better and also excelled in reproducing some of the helical parameters.[5] Here we present the first application of MD-tar to a DNA fragment using real experimental data. The structure of [d(GTATAATG]·[d(CATATTAC)], recently determined with standard rMD,[6] was taken as the starting point to explore conformational space with both conventional rMD and MD-tar simulations[7] in relatively long trajectories of 120 ps—still short for MD-tar.[5]

Conformational sampling with standard rMD and MD-tar is indeed quite different. The atomic root-mean-square deviation (rmsd) between 20 superimposed snapshots taken every 5 ps was 0.77 Å for standard rMD and 2.27 Å for MD-tar calculations. With an rmsd for an unrestrained MD simulation of 1.37 Å, the conformational envelope of MD-tar seems more realistic. However, local excursions from double-helical geometry, e.g., base-pair opening and closing and fraying of terminal base pairs, were observed in MD-tar simulations; this agrees with experiment but occurs on a much faster time scale. Apparently, simulations using time-averaged restraints can explore conformational space available to the molecule on a slower time scale.

More realistic conformational sampling is also evident for intranucleotide geometries, e.g., sugar pucker and glycosidic torsion angle. Our independent pucker analysis of 2QF-COSY data showed that none of the deoxyribose rings existed in a single conformational state.[6] Rather, the 2QF-COSY data could be accounted for by two-state dynamic mixtures entailing a major conformer with a pucker value in the S-range (population 70–100%, pseudorotation phase angle P = 126–180°) and a minor conformer with fixed geometry (P = 9°). Whereas standard rMD arrives at a single structure, which is a compromise between matching all restraints and minimizing energy, MD-tar can accommodate sugar repuckering. Indeed, in our simulations, all deoxyribose rings undergo conformational flips between S- and N-regions, with 67–97% populations for the S-conformer. Even a reasonable correlation between sugar pucker and glycosidic torsion angle[8] could be reproduced in our MD-tar simulations (Figure 1).

The ultimate criterion for improved conformational sampling, however, lies in comparison with the experimental 2D NOE data. We calculate theoretical 2D NOE spectra for a structure by complete relaxation matrix analysis with the program CORMA,[9,10] and we compare the match of theoretical to experimental 2D NOE intensities via residual indices R and R^x, where R is the equivalent of the crystallographic R-factor and R^x is a variation entailing sixth-root weighting of intensities to avoid domination by short distances:[11] $R^x = \sum_i |I_o^{1/6}(i) - I_c^{1/6}(i)| / \sum_i |I_o^{1/6}(i)|$, where $I_o(i)$ is the experimental and $I_c(i)$ is the corresponding calculated intensity of cross-peak i for a particular structure.[12] We recently modified CORMA so that R and R^x can be calculated for a rapidly interchanging ensemble of structures; relaxation rates of individual snapshots are averaged, and the resulting theoretical intensity matrix is compared with experimental intensities. This is distinct from comparing arithmetically averaged intensities for a set of structures. For the present study, we calculated residual indices for the central six base pairs of the octamer using 100 snapshots each (last 100 ps) for both standard rMD and MD-tar simulations compared with 100- and 150-ms 2D NOE data. Both data sets yielded essentially the same results, and the crystallographic R-factor largely mirrored the structurally more sensitive sixth-root R-factor. While the simple arithmetic average of intensities produced R^x values of 0.121 vs 0.071 for the MD-tar vs standard rMD set of structures, the relaxation-rate-averaged R^x values were 0.053 vs 0.066 (150-ms data). The significant difference between the arithmetic and relaxation-rate ensemble averages for MD-tar demonstrates that it is the ensemble as a whole that satisfies the NOE data rather than the compromised fit of snapshots. The ensemble R-factors resulting from MD-tar are the lowest R-values we have ever obtained for the octamer, indicating that no single standard rMD snapshot is a better match than the MD-tar ensemble. While most average structural parameters obtained from both methods are largely the same, a reasonable structural analysis of an ensemble requires scrutinizing distributions of structural

(2) Torda, A. E.; Scheek, R. M.; van Gunsteren, W. F. *Chem. Phys. Lett.* **1989**, *157*, 289–94.
(3) Torda, A. E.; Scheek, R. M.; van Gunsteren, W. F. *J. Mol. Biol.* **1990**, *214*, 223–235.
(4) Pearlman, D. A.; Case, D. A.; Caldwell, J. C.; Seibel, G. L.; Singh, U. C.; Weiner, P.; Kollman, P. A. *AMBER4* (*UCSF*); University of California: San Francisco, 1991.
(5) Pearlman, D. A.; Kollman, P. A. *J. Mol. Biol.* **1991**, *220*, 429–457.
(6) Schmitz, U.; Sethson, I.; Egan, W.; James, T. *J. Mol. Biol.* **1992**, *227*, 510–531.
(7) The in vacuo calculations utilizing the all-atom AMBER force field (Weiner, S. J.; Kollman, P. A.; Nguyen, D. T.; Case, D. A. *J. Comput. Chem.* **1986**, *7*, 230–252) consisted of 120 000 steps in 1-fs increments with a nonbonded cutoff distance of 12 Å, a distance-dependent dielectric, and implicit solvent counterions (Rao, S. N.; Singh, U. C.; Kollman, P. A. *Isr. J. Chem.* **1986**, *27*, 189–197). SHAKE (Ryckaert, J. P.; Cicotti, G.; Berendsen, H. J. C. *J. Comput. Phys.* **1977**, *23*, 327–341) was used to constrain all covalent bond lengths and angles. The simulations were kept at a constant temperature by coupling to a temperature bath (Berendsen, H. J. C.; Postma, J. P. M.; van Gunsteren, W. F.; Di Nola, A.; Haak, J. R. *J. Chem. Phys.* **1984**, *81*, 3684–3690) with different scaling for counterions and for the DNA. Force constants were 25 kcal/mol·Å^2 for all interproton distances and 12.5 kcal/mol·Å^2 for Watson–Crick hydrogen-bond restraints. For both simulations, the starting structure was generated from the previously reported final structure (Schmitz, U.; Sethson, I.; Egan, W.; James, T. *J. Mol. Biol.*, in press) by heating to 300 K and equilibrating for 30 ps with the requisite force constants. For MD-tar simulations, "pseudoforces" with an exponential decay constant τ = 10 ps for weighting the history of snapshots were used to evaluate the distance penalty (Torda, A. E.; van Gunsteren, W. F. *Comp. Phys. Commun.* **1991**, *62*, 289–296; Knegtel, J. M. A.; Boelens, R.; Ganadu, M. L.; Kaptein, R. *Eur. J. Biochem.* **1991**, *202*, 447–458). For distance averaging, a third-root weighting was used (Tropp, J. *J. Chem. Phys.* **1980**, *72*, 6035–6043). Structural analysis was carried out on 400 snapshots acquired every 0.25 ps over the last 100 ps of each simulation utilizing the program *Dials & Windows* (Ravishanker, G.; Swaminathan, D. L.; Beveridge, D. L.; Lavery, R.; Sklenar, H. *J. Biomol. Struct. Dyn.* **1989**, *6*, 669–699).

(8) Fratini, A. V.; Kopka, M. L.; Drew, H. R.; Dickerson, R. E. *J. Biol. Chem.* **1982**, *257*, 14686–14707.
(9) Keepers, J. W.; James, T. L. *J. Magn. Reson.* **1984**, *57*, 404–426.
(10) Borgias, B. A.; James, T. L. *J. Magn. Reson.* **1988**, *79*, 493–512.
(11) Thomas, P. D.; Basus, V. J.; James, T. L. *Proc. Natl. Acad. Sci. U.S.A.* **1991**, *88*, 1237–1241.
(12) James, T. L.; Gochin, M.; Kerwood, D. J.; Pearlman, D. A.; Schmitz, U.; Thomas, P. D. In *Computational Aspects of the Study of Biological Macromolecules by Nuclear Magnetic Resonance Spectroscopy*; Hoch, J. C., Poulsen, F. M., Redfield, C., Eds.; Plenum Press: New York, 1991; pp 331–348.

parameters. A detailed study is in progress.

Acknowledgment. This work was supported by National Institutes of Health Grants GM41639 and GM39247. We thank Dr. D. L. Beveridge for kindly providing *Dials & Windows*. We gratefully acknowledge discussions with J. Guenot and Drs. D. A. Pearlman and N. B. Ulyanov, the use of the UCSF Computer Graphics Laboratory (supported by NIH Grant RR 01081), and the Cray X-MP supercomputer at the MSI, University of Minnesota.

A Polyester and Polyurethane of Diphenyl C_{61}: Retention of Fulleroid Properties in a Polymer

S. Shi, K. C. Khemani, Q. "Chan" Li, and F. Wudl*

Institute for Polymers and Organic Solids
Departments of Chemistry and Physics
University of California, Santa Barbara, California 93106

Received August 17, 1992

Buckminsterfullerene, C_{60},[1] and its unusual chemical properties,[1b,2] in particular the fulleroid synthesis,[1b,3] prompted us to investigate the possibility of preparing polymers[4] containing the C_{60} moiety as either a member of the backbone ("pearl necklace") or a pendant group ("charm bracelet").[5] We describe herein the syntheses and characterization of two charm-bracelet-type polymers containing C_{61} molecules dangling from the polymer backbone.

The polymers were prepared according to Scheme I, and the monomer synthesis is shown in Scheme II.

$(HOC_6H_4)_2C_{61}$ (**1**) is very stable in pyridine, partially soluble in ether, tetrahydrofuran, or *o*-dichlorobenzene, and only very sparingly soluble in benzene or toluene.

Polymerization of **1** and sebacoyl chloride in dry nitrobenzene at 143 °C (22 h), using equimolar amounts of the monomers and no catalyst,[7] produced poly(4,4'-diphenyl-C_{61} sebacate), **2**, in 61% yield as a brown powder[8] which was sparingly soluble in THF but soluble in nitrobenzene and benzonitrile. Infrared spectroscopy of a KBr pellet of the polymer showed the presence of sp^3 C—H (2920, 2850 cm^{-1}) and ester C=O (1760, 1725 cm^{-1}) stretching vibrations. The ^1H NMR spectrum in THF-d_8 had peaks at 10.83 ppm (suggesting the presence of an OH end group), 6.8–8.55 ppm (several sets of sharp peaks: multiplets, phenylene protons), and 1.2–2.6 ppm (several peaks; multiplets, hexamethylene protons).

Comparative thermogravimetric analysis (TGA) results for **1**, poly(biphenol A sebacate) (PBAE), and **2** revealed that, as is the case with most C_{61} fulleroids, **1** is moderately thermally stable. It gradually loses weight upon heating, retaining ~90% of its original mass at 500 °C and ~83% at 700 °C. PBAE exhibits a rapid weight loss from 360 to 480 °C (95% of its initial mass). Similar to PBAE, the TGA of **2** also reveals a weight loss between 360 and 480 °C. Only about 9% (calculated 15.5%) weight loss for the decomposition of **2** was observed in that temperature range.[9] Apparently decomposition to volatile fragments is far from quantitative.

Scheme I

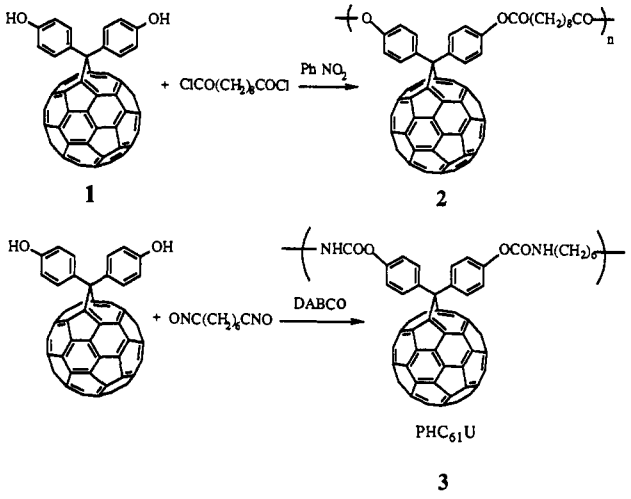

Scheme II[a]

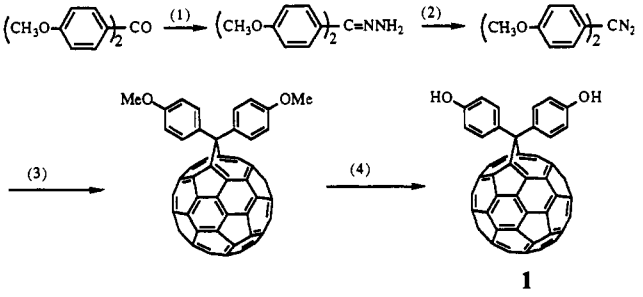

[a] (1) NH_2NH_2/ethanol, reflux,[6] 86%; (2) HgO/petroleum ether, room temperature; (3) C_{60}/toluene, room temperature, 73%; (4) BBr_3/*o*-dichlorobenzene, 0 °C to room temperature, 94%.

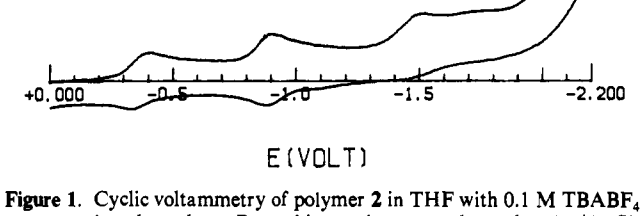

Figure 1. Cyclic voltammetry of polymer **2** in THF with 0.1 M $TBABF_4$ as supporting electrolyte: Pt working and counter electrodes; Ag/AgCl, reference electrode; scan rate, 100 mV/s.

The UV–vis spectrum of a THF solution of **2**, while showing broad bands, is reminiscent of other C_{61}'s[3] with bands at 690, 475, 430, 330, 275, and 250 nm. Solution cyclic voltammetry of the polymer in THF is shown in Figure 1. The presence of the first three characteristic reduction waves[3] of all diphenyl C_{61}'s clearly shows that the polymer retained the electronic properties of diphenyl fulleroids.

When an equimolar amount of hexamethylene diisocyanate and **1** in *o*-dichlorobenzene was heated in the presence of a catalytic amount of 1,4-diazabicyclo[2.2.2]octane (DABCO), an insoluble, brown powder was obtained in 60% yield.[10]

(1) (a) Krätschmer, W.; Lamb, L. D.; Fostiropoulos, K.; Huffman, D. R. *Nature* **1990**, *347*, 354. (b) *Acc. Chem. Res.* **1992**, *25*, 1–200.

(2) *Fullerenes Synthesis, Properties, and Chemistry of Large Carbon Clusters*; Hammond, G., Kuck, V. J., Eds.; ACS Symposium Series 481; American Chemical Society: Washington, DC, 1992.

(3) Suzuki, T.; Li, Q.; Khemani, K. C.; Wudl, F.; Almarsson, Ö. *Science* **1991**, *254*, 1186.

(4) (a) Polymers containing a C_{60} unit in the backbone of a poly(*p*-xylylene) have recently been reported by Loy, D. A., and Assink, R. A., presented at the Materials Research Society Meeting, Boston, Dec 1991. (b) A "fullerenated" poly(styrene) was prepared by Prakash and Olah: Prakash, S.; Olah, G. *J. Am. Chem. Soc.*, in press.

(5) Amato, I. *Science* **1991**, *254*, 30 quoting F. Wudl.

(6) Snyder, H. R.; Rowland, R. L.; Sampson, H. J., Jr. *Organic Syntheses*; Wiley: New York, 1955; Collect. Vol. III, p 351.

(7) HCl was removed by bubbling nitrogen through the reaction mixture.

(8) Contrary to **2**, **3** did not produce good, reproducible combustion analysis results. Attempts are being made to correct this problem. Other analytical data are in accord with the proposed structure. Both polyesters had low M_w. GPC (polystyrene standard) M_w 4000; $[\eta] = 0.2 \pm 0.1$ dL/g (0.9 g/dL).

(9) The weight loss between 200 and 360 °C is typical of diphenyl fulleroids and has not been assigned to any particular fragmentation.

0002-7863/92/1514-10656$03.00/0